

# EFFECT OF GLYCEROL ON THE ELECTRICAL PROPERTIES AND PHASE BEHAVIOR OF CASSAVA STARCH BIOPOLYMERS

## EFEECTO DEL GLICEROL SOBRE LAS PROPIEDADES ELÉCTRICAS Y COMPORTAMIENTO DE FASE EN BIOPOLÍMEROS DE ALMIDÓN DE YUCA

GERMÁN AYALA

*Ingeniero Agroindustrial. Universidad Nacional de Colombia, sede Palmira, gayalav@usp.br*

ANA AGUDELO

*PhD. Facultad de Ingeniería y Administración, Universidad Nacional de Colombia, sede Palmira, acagudeloh@unal.edu.co*

RUBÉN VARGAS

*PhD. Facultad de Ciencias Naturales y Exactas, Universidad del Valle, ruben.vargas@correounivalle.edu.co*

Received for review April 4<sup>th</sup>, 2011, accepted August 3<sup>th</sup>, 2011, final version August, 12<sup>th</sup>, 2011

**ABSTRACT:** Films of different concentrations of glycerol/starch (G/S) blends were prepared and analyzed by impedance spectroscopy (IS), differential scanning calorimeter (DSC) and thermogravimetric analysis (TGA). The dc-conductivity of the films increases by increasing both the glycerol content and temperature. A power-law dispersive behavior of the frequency-dependent conductivity at high frequencies has been observed in all G/S films in the blend compositions prepared, similar to that observed in other solid ionic conductors and known as a “universal dynamic response.” The electrical conductivity enhancement is consistent with the subtle changes in the -OH glycerol groups coordination with the starch chains introduced by increasing the glycerol content and temperature. A stable single phase is revealed under the electrical measurement conditions up to approximately 100 °C for all concentrations, but the stability can be maintained up to higher temperatures (~150 °C) at glycerol concentrations below G/S = 0.4.

**KEY WORDS:** cassava starch, glycerol, electrical conductivity, phase behavior

**RESUMEN:** Se prepararon películas de diferentes concentraciones de glicerol/almidón (G/S) y se caracterizaron a través de espectroscopía de impedancia (IS), calorimetría diferencia de barrido (DSC) y termogravimetría (TGA). La conductividad dc de las películas incrementó con el incremento en el contenido de glicerol y la temperatura. La dependencia de la conductividad con la frecuencia mostró un comportamiento de ley de potencia a altas frecuencias para todas las películas, similar al que se observa en otros conductores iónicos sólidos, el cual es conocido como “respuesta universal.” El incremento en la conductividad eléctrica es consistente con el aumento en grupos -OH a medida que se incrementa el contenido de glicerol y la temperatura. Para todas las concentraciones, y bajo las condiciones de las medidas eléctricas, se observó una fase estable hasta aproximadamente 100 °C; la estabilidad se mantiene hasta temperaturas del orden de 150 °C a concentraciones de glicerol por debajo de G/S = 0.4.

**PALABRAS CLAVE:** almidón de yuca, glicerol, conductividad eléctrica, comportamiento de fase

### 1. INTRODUCTION

In recent years, the analysis of natural polymers derived from renewable sources, such as starch, has gained importance [1]. Many studies have been conducted to understand the various properties of the films produced from this biopolymer [2-6].

The industrial use of starch is based on its biodegradable nature, low cost and abundance in availability [3]. It can be used as a polymeric matrix in short shelf life

products [7]. Starches can have different grades of semi-crystallinity and grain size depending on their botanical source [8,9]. Starches from corn, cassava, wheat, or rice are commercially available and have specific properties that suit many applications at the industrial level [10]. The production process of biopolymers is based on plasticizing the native starch in the presence of a plasticizer rich in hydroxyl groups such as glycerol [11,12]; nevertheless, the plasticizing effect of some other compounds such as water, citric acid, and some polyalcohols, have also been analyzed [2,6,13,14].

The plasticizer increases the flexibility of the film due to its capacity to reduce the amount of internal hydrogen links between polymer chains, thereby reducing the glass transition temperature ( $T_g$ ) [15,16]. Due to the flexibility of these biopolymers, their main applications are in the field of surface plastic coverings such as capsules and low humidity environment packing [17]; nevertheless, it is probable that depending on the nature of the plasticizer, the electrical conductivity of the biopolymer would increase, thus opening the path to new applications such as solid polymer electrolytes. This functionality has attracted much attention in recent years for its use in a variety of electrochemical applications such as humidity sensors, rechargeable batteries, and fuel cells [18,19].

The objective of this study is to assess the effect of glycerol on the electrical and thermal properties of cassava starch plastic films. Earlier investigations have reported that the addition of polyalcohol such as glycerol or ethylene glycol improves the conductivity of various polymeric systems [20]. With the objective of understanding the ionic conduction mechanisms and their relations to the phase behavior of glycerol/starch films, this paper investigates the effect of the synthesis route on the dynamics of ionic conduction, which are examined as a function of the temperature and frequency of the applied electric field. Special emphasis is put on the dependence on water content in partially hydrated membranes. As a matter of fact, the usual polymer electrolyte membranes such as Nafion® (developed by DuPont de Nemours, USA, in the 1960s) are somewhat unusual electrolytes in that, in the presence of water, which is readily absorbed by the membranes, they become highly ionic conducting materials. However, the most significant drawbacks of these commercially available proton-exchange membranes (PEMs) are the relatively high cost, the dependence on high levels of water content for conduction, and instability at temperatures in excess of 100 °C.

## 2. MATERIALS AND METHODS

### 2.1 Materials

Cassava starch HMC 1 was supplied by the International Center of Tropical Agriculture (CIAT), Colombia. The cassava was planted in the southwest of Colombia, in the Valle del Cauca province. The moisture content of the starch was determined by drying the sample in an air-oven at 105 °C for 24 h until constant weight and

the value was  $13.7 \pm 0.3$  wt % (wet basis). Glycerol commercial grade was 99 %.

It is important to point out that the cassava starch used to prepare the membranes was initially gelatinized using an aqueous solution of 3.0 wt % concentration at  $70 \pm 0.5$  °C. If the solution was instead thermally treated at temperatures lower than 62 °C, then semi-crystalline starch granules precipitate from the solution. Even more, as it was previously reported [21], at about 62 °C, amylase starts to escape from the solution; and, as a consequence, the viscosity of the resulting gel increases considerably.

### Preparation of glycerol/cassava starch films

Glycerol/ starch films at various concentrations were prepared by using a previously reported solution casting method [17,22,23]. As was described above, the cassava starch was previously gelatinized at  $70 \pm 0.5$  °C during 15 min under a constant agitation of 250 rpm. Glycerol, which acts as a plasticizer, was added in different proportions into identical starch suspensions in beakers at  $70 \pm 0.5$  °C and treated at this temperature during an additional 15 min under a constant agitation of 250 rpm. The mixtures with a gel texture were then spread over Teflon containers and dried at 50 °C for 18 hours in a SASSIN mlw oven, until they became solid. We obtained smooth, uniform in thickness, semitransparent to the visible light, and thin membranes.

The thickness of the resulting films was done in triplicate and was determined with a precision micrometer (Mitutoyo Tokyo, Japan). It varied between 0.06 and  $0.17 \pm 0.01$  mm. The films were stored in desiccators with silica gel for a period of 96 hours and then transferred in sealed polyethylene bags to the various instruments for analysis. We prepared five Glycerol/Starch (G/S) concentrations, in the weight ratio, G/S = 0.1, 0.2, 0.3, 0.4 and 0.5, respectively.

### 2.2 Films characterization

#### 2.2.1 Moisture Determination

The moisture content of the films with the concentrations prepared was determined following the AOAC (1990) standard [24], by drying the sample in an air-oven at 105 °C for 24 hours until constant weight was reached; this determination was performed at least twice.

### 2.2.2 Impedance Spectroscopy (IS)

The electrical measurements were made for glycerol/cassava polymer films by an ac impedance method. The polymer membranes were sandwiched between SS304 stainless steel, ion-blocking electrodes, each of a surface area of 0.785 cm<sup>2</sup>, in a spring-loaded stainless steel holder. The measuring cell was located in a sealed, temperature-controlled chamber [25]. A Pt 100 temperature sensor was kept close to the G/S polymer membrane for temperature measurement. Each sample was equilibrated at the experimental temperature for at least 2 min before measurement. The complex impedance measurements were carried out using a LCR meter (Wayne Kerr 6420, New Boston, USA) controlled by a computer, in the frequency range from 20 Hz to 3 MHz at an excitation signal of 100 mV. Possible nonlinear effects were checked at amplitudes of up to 500 mV over the entire frequency range for a typical cell. The impedance of the composite polymer membrane was recorded at various isotherms in the temperature range between 30 and 150 °C. All sweeps were carried out in a sealed chamber. The experimental temperatures were maintained within  $\pm 0.1$  °C by the temperature-control of the shielded chamber. All polymer membranes were studied at least three times.

### 2.2.3 Thermogravimetric Analysis (TGA)

The TGA measurements were made using a thermogravimetric analyzer (TGA 2920 TA Instruments, New Castle, DE, USA), under a flow of dry N<sub>2</sub> (50 ml/min). The films were weighed directly into an aluminum pan (2–3 mg). The pans were heated from 30 to 330 °C at a rate of 10 °C/min. The weight loss and weight derivatives were determined from the TGA curves by means of the Universal Analysis 2000 software provided by the TA Instruments Company. All G/S polymer membranes were studied at least three times.

### 2.2.4 Differential Scanning Calorimeter (DSC)

The DSC measurements were made using a modulated differential scanning calorimeter (MDSC 2920 TA Instruments, New Castle, DE, USA) under a flow of dry N<sub>2</sub> (50 ml/min). Films were weighed directly into an aluminum pan (3–5 mg), which was hermetically sealed. An aluminum empty pan was used as a reference. The pans were heated from -20 °C to 300

°C at a rate of 10 °C/min. The calibrations of the DSC temperature and heat flow were done according to the standard ASTM (D-3418) [26], using the pure indium (melting point 156.4 °C) with the same heating rate used for the DSC measurements (10 °C/min). The transition temperatures (onset, T<sub>o</sub>; peak, T<sub>p</sub>; and conclusion, T<sub>c</sub>) of the observed thermal events were determined from the DSC curves by means of the Universal Analysis 2000 software provided by the TA Instruments Company. Calorimetric enthalpy ( $\Delta H$ ) associated with the thermal events was determined by numerical integration of the area under the peak of thermal transition. All G/S polymer membranes were studied at least three times.

## 3. RESULTS

### 3.1 Moisture Determination

The moisture content of the glycerol/starch (G/S) films with concentrations G/S = 0.1 and G/S = 0.2 was  $7.3 \pm 0.1$  wt % (wet basis), and that of the films with concentrations G/S = 0.3, G/S = 0.4, and G/S = 0.5 was  $10.1 \pm 0.1$  wt %.

### 3.2 Impedance Spectroscopy

Impedance spectra of films gave Nyquist plots. Figure 1 shows several typical (-ImZ vs. ReZ) plots taken at T = 30, 70, 100, 110, 130, and 150 °C for the film G/S = 0.3. Note that the Nyquist plots show in the operating frequency range a well-defined arc passing through the origin in the high frequency limit, which is related to the conduction process in the bulk of the films. It can also be noticed that the extrapolation of the arc to the ReZ axis, whose intercept is the bulk resistance of the film, R, decreases with increasing temperature, thus showing some kind of thermal activated process.

The dc conductivity,  $\sigma$ , was calculated from the Nyquist plots as usual, using the formula,  $\sigma = d/AR$ , where d is the thickness, and A is the contact area of the film; R is obtained from the intercept of the arc with the ReZ axis, as indicated above. Figure 2 shows the temperature dependence of the dc-conductivity for the G/S films in the blend compositions prepared, plotted as Log  $\sigma$  vs. 1000/T. Based on the least square analysis of the corresponding data, they were better fitted to the Arrhenius rather than to the VTF (Vogel-

Tamman-Fulcher) type-models, if two segments, one at low temperatures and another one at high temperatures, are selected (see Fig. 2-b for a representative fitting for the dc-conductivity data of the G/S = 0.4 film). The activation energy,  $E_a$ , is calculated from the fitting parameters. according to the Arrhenius model,  $\ln\sigma = \ln\sigma_0 - E_a/k_B T$ , where  $k_B$  is the Stefan Boltzmann's constant (8.6171E-5 eV/K). Table 1 gives the activation energy for all the G/S film compositions prepared, in two temperature ranges: 50–80 °C ( $E_{a1}$ ) and 90–150 °C ( $E_{a2}$ ), respectively, for the compositions G/S = 0.1, 0.2, and 0.3; while in the case of those for G/S = 0.4, the data were fitted in temperatures ranges 30–90 °C ( $E_{a1}$ ), and 100–150 °C ( $E_{a2}$ ), respectively. However, the data for G/S = 0.5 were analyzed only in the low-temperature region, 30–100 °C ( $E_{a1}$ ), since at higher temperatures the sample showed high thermal instability. Note that the activation energy in the high temperature region is lower than that of the low-temperature region, except for the sample with the lowest glycerol

content (G/S = 0.1). This change in slope is often observed in polymer electrolytes [27,28] and it is generally associated with a thermal change in the polymeric complex, between two different elastomeric phases with different water content.

It is important to stress that the VTF-type thermal activated process of the dc conductivities is usually observed for dehydrated polymer electrolytes, in which the dominant mechanism for ion transport depends on the chain motion of polymers. However, when the polymers are hydrated, the dc conductivity is better fitted to an Arrhenius-type model, as is the case in the present work.

Figure 3 shows the dependence of the dc-conductivity on glycerol concentration, G/S, in which  $\sigma$  vs. glycerol content is plotted at several isotherms. Increasing the temperature and concentration of glycerol, the dc-conductivity increases. The highest

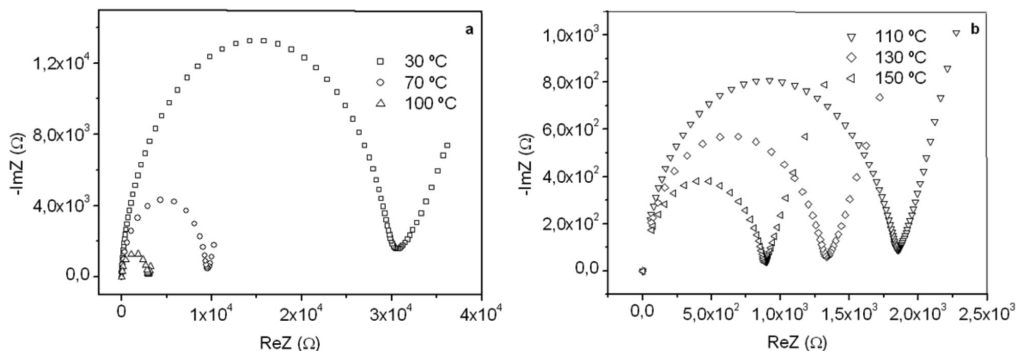


Figure 1. Representative impedance plots for the G/S = 0.3 film at 30, 70, 100 °C (a), and 110, 130, 150 °C (b)

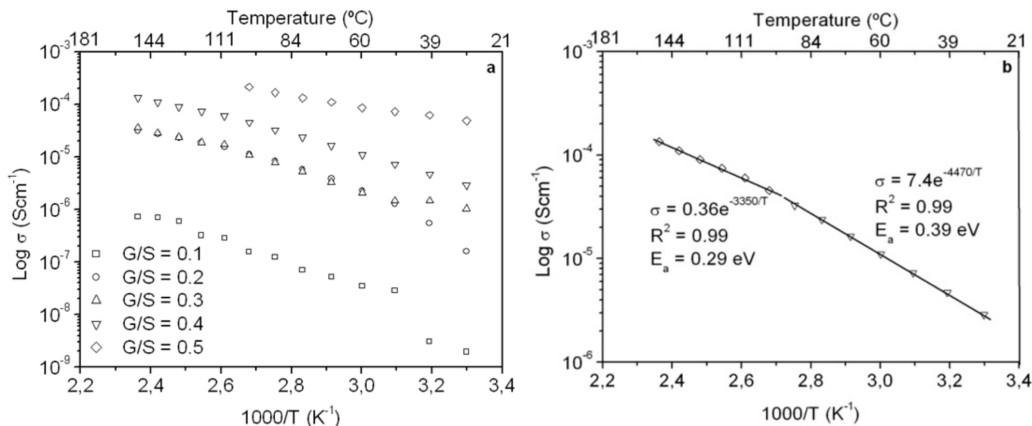
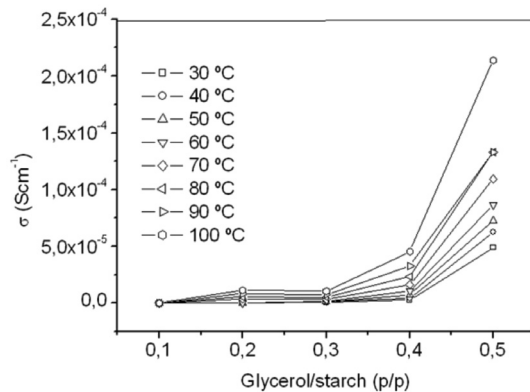


Figure 2. Log dc-conductivity vs. inverse temperature plots for the G/S films (a), and Log dc-conductivity vs. inverse temperature plot for the G/S = 0.4 film. Solid lines are linear fittings to the Arrhenius model  $\ln\sigma = \ln\sigma_0 - E_a/k_B T$  (b)

**Table 1.** Arrhenius activation energy,  $E_a$ , for the G/S films. The energy of activation was calculated as the product between the slope of the mathematical model by (-1), by Stefan Boltzmann's constant ( $K_B$ )

Films	First fitting			Second fitting		
	Mathematical model	$E_a$ (eV)	$R^2$	Mathematical model	$E_a$ (eV)	$R^2$
G/A = 0.1	$\sigma = 1E-3e^{-3520/T}$	3.03 E-01	0.98	$\sigma = 1E-1e^{-4950/T}$	4.27 E-01	0.96
G/A = 0.2	$\sigma = 91.4e^{-5830/T}$	5.02 E-01	0.99	$\sigma = 8.6E-2e^{-3330/T}$	2.87 E-01	0.99
G/A = 0.3	$\sigma = 5.8e^{-4920/T}$	4.24 E-01	0.99	$\sigma = 3E-1e^{-3800/T}$	3.27 E-01	0.98
G/A = 0.4	$\sigma = 7.4e^{-4470/T}$	3.85 E-01	0.99	$\sigma = 3.6E-1e^{-3350/T}$	2.88 E-01	0.99
G/A = 0.5	$\sigma = 9.8E-2e^{-2331/T}$	1.90 E-01	0.99	-----	-----	-----

conductivity value,  $2.13 \text{ E-}04 \text{ Scm}^{-1}$ , is that of the G/S = 0.5 film, found at  $100 \text{ }^\circ\text{C}$ . Thus, the ionic conductivity of the prepared G/S films are in the range of the typical solid electrolytes, such as ionic crystals, glasses, composites, and polymer-salt complexes, which lie in the range of  $10^{-6} \leq \sigma \leq 10^{-1} \text{ Scm}^{-1}$ , a characteristic of dilute ionic solutions [17,18].



**Figure 3.** Dc-conductivity vs. glycerol concentration plots at eight different temperatures

We have dealt so far with the dc-conductivity of the G/S films and its dependence on glycerol concentration and temperature. Much effort has also been devoted during the last few decades to understanding the dynamics of ionic transport in ionic conducting materials. One of those research activities is focused on the origin and properties of the long-range ion motion, and electrical relaxation is the most commonly used experimental tool used to access ion dynamics. Figure 4 shows typical plots of the frequency dependence of the real part of the conductivity,  $\sigma'(\omega)$ , for the G/S = 0.3 film, presented in a double-logarithmic scale at several isotherms (the ac-conductivity,  $\sigma(\omega) = \sigma'(\omega) + i\sigma''(\omega)$ , was calculated from the complex admittance data,

$Y(\omega) = 1/Z(\omega) = G(\omega) + i\omega C(\omega) = (A/d)\sigma(\omega)$  where  $G$  and  $C$  are the parallel conductance and capacitance, respectively). Power-law dependence seems to appear in Fig. 4 at the high frequency range, which is quite evident at lower temperatures; and a crossover to a frequency independent dc regime (dc-conductivity plateau), occurs at low frequencies. The crossover defines a characteristic relaxation frequency,  $\omega_p$  which increases with increasing temperature. The observed dispersive behavior of the frequency-dependent conductivity at high frequencies has been interpreted as a result of the many body interactions between charge carriers. It is important to stress that the values of  $\sigma'(0)$ , obtained by the extrapolation of the dc-conductivity plateau (low-frequency region) shown in Fig. 1, coincide within the experimental error with those obtained by using the values of  $R$  given by the Nyquist plots (Fig. 1), by extrapolating the circular arc to the real axis of the impedance plots.

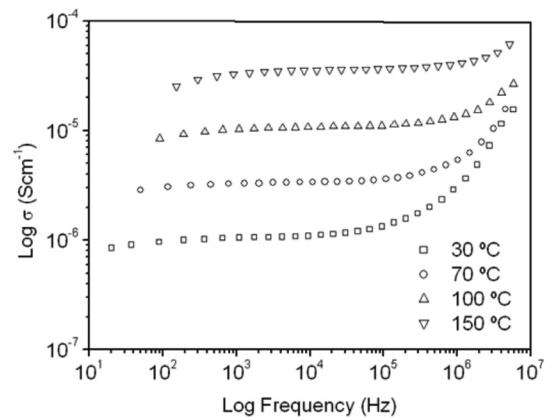


**Figure 4.** Real part conductivity vs. frequency for the G/S = 0.3 film, presented in a double logarithmic scale at several temperatures

Identical results to those reported for the G/S = 0.3 film in Fig. 4 were found for all films. These profiles have been widely observed in highly structural disordered materials like ionic conducting glasses, conducting polymers, amorphous semiconductors, and doped crystalline solids [29]. This feature is often referred to as “universal dynamic response.” Thus, these observations indicate that charge transfer mechanisms based in ion migration mediated by either ion-ion or ion-polymer chain interactions, similar to those found in other ionic materials, are also responsible for ionic conductivity in the G/S polymeric complexes.

### 3.3 TGA thermal analysis

Figure 5 shows TGA (a) and differential gravimetric analysis (DTG) (b) curves of the G/S polymer films prepared. The TGA and DTG curves of the G/S = 0.5 polymer film reveal three main weight loss regions. The first region in the 30–100 °C temperature range is due to the evaporation of physical weakly and chemically strongly bound water; the total weight loss of the membrane is about 10 wt % at 100 °C. The second transition region in the 100–230 °C temperature range, which also appear as a peak in the DTG curves is due to the degradation of glycerol in the polymer membrane; the total weight loss corresponds to this stage about 23 wt % at 230 °C. The third peak at about 300 °C is due to the degradation backbone of starch polymer membrane; there is a total weight loss of about 78 wt % at 327 °C.

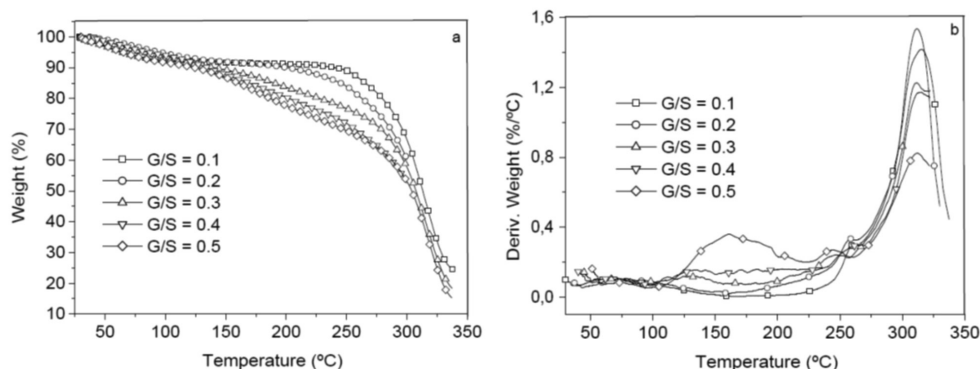


**Figure 5.** TGA (a), and differential gravimetric analyzer curves DTG (b), for the G/S films

total mass of the sample. It should be emphasized that the measured enthalpy corresponds to the total energetic of the biopolymer molecular interactions, i.e., of the starch + glycerol + water constituents (gel type

Furthermore, the TGA and DTG curves for the rest of the G/S polymer films with less glycerol content (G/S = 0.1, 0.2, 0.3, and 0.4) also exhibit three main weight loss regions. The first stage, similar to that of the G/S = 0.5 film, e.g., is shown in the 30–100 °C temperature range, as well the fact that due to the evaporation of water and the total weight loss, it is about 10 wt % at 100 °C. However, in the second transition region, which is also shown between 100 and 230 °C for all polymer films, no peak in the DTG curves are observed; but the rate of weight loss with temperature increases with increasing glycerol content, due to the degradation of glycerol in the polymer films. Similar to the TGA curve for the G/S = 0.5 film, the third region shows a peak at about 300 °C which is due to the degradation backbone of the starch polymer membrane and there is also a total weight loss of about 78 wt % at 327 °C.

### 3.4 DSC thermal analysis

Figure 6 shows a plot of heat flow vs. temperature between 10 and 240 °C obtained by differential scanning calorimeter (DSC) for the G/S polymer films equally hydrated as shown by the TGA curves (Fig. 5). A broad endothermic peak between approximately 30 and 150 °C is observed in the DSC curves on heating for all G/S films concentrations which is associated with water content in the films and its interaction with the polymer matrix (starch + glycerol). Table 2 summarizes the change of enthalpy ( $\Delta H$ ) and the corresponding peak's temperature for each G/S concentration. The enthalpies are given in J/g by dividing the enthalpy obtained from the DSC data by the

biopolymer) and not for the starch component only. It is found that  $\Delta H$  decreases as the glycerol content increases in the G/S films with concentrations of up to G/S = 0.4 indicating that water molecules are less bound

when the glycerol concentration increases. However, for the  $G/S = 0.5$  films,  $\Delta H$  increases again because of the contribution of the enthalpy associated with the degradation of glycerol. It should be stressed that in the whole operating temperature of the DSC measurements (from  $-20$  to  $300$  °C), no other thermal event was observed in the DSC curves in the temperature ranges between  $-20$  and  $30$  °C as well as between  $150$  and  $300$  °C, except for the exothermic events that start to appear at about  $240$  °C, associated with the degradation backbone of starch polymer membrane.

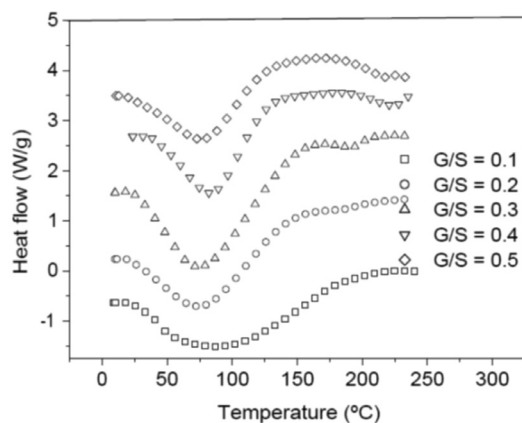


**Figure 6.** DSC curves for the G/S films

**Table 2.** Change of the enthalpy ( $\Delta H$ ) and the transition temperatures for the G/S films

Films	$T_o$ (°C)	$T_p$ (°C)	$T_c$ (°C)	$\Delta H$ (J/g wet matter)
G/S = 0.1	$22 \pm 0.3$	$77 \pm 0.2$	$179 \pm 1.2$	$219 \pm 16.0$
G/S = 0.2	$21 \pm 0.3$	$77 \pm 0.1$	$145 \pm 0.9$	$162 \pm 9.2$
G/S = 0.3	$21 \pm 0.6$	$77 \pm 0.2$	$146 \pm 0.4$	$159 \pm 7.2$
G/S = 0.4	$34 \pm 2.1$	$84 \pm 0.3$	$137 \pm 2.3$	$148 \pm 11.3$
G/S = 0.5	$19 \pm 0.8$	$85 \pm 1.3$	$127 \pm 4.2$	$171 \pm 5.0$

#### 4. DISCUSSION

The effects of adding glycerol, which is rich in hydroxyl groups and acts as a plasticizer, to the cassava starch were mainly on increasing dc electrical conductivity of the prepared biopolymer films, where the film  $G/S = 0.3$  present the critical concentration on the increase dc-conductivity (see Fig. 3), which may be due to the increased presence of hydroxyl groups in the films. Its addition, it was also important to reduce the biopolymer intermolecular forces, the mobility of its polymeric chains, and to improve the mechanical characteristics of the resulting film, such as the film extensibility [30].

The concentrations of plasticizer were chosen based on our preliminary experiments and the reproducibility of the electrical measurements, which are very sensitive to the homogeneous incorporation of it, as well as to the water content in the films. In fact, when the films are equilibrated in an open cell at a high relative humidity ( $\sim 70$  RH %), we observed that the ionic conductivity steadily decreases when temperature is increasing, due to the evaporation of water from the films. This is why special attention was placed on maintaining the water content in the films for the electrical measurements constant, and since the conductivity vs. temperature sweeps act as a heat treatment (that diminish this water content). Besides, the sample geometry and the cell configuration used for the electrical measurements helped to control the water evaporation at a very low level during the data acquisition. Therefore, the data in Figs. 1–4 reflect the increase of the ionic transport with increasing temperature at almost constant water content or in a single phase, which is stable in a wide range of temperatures above room temperature, depending on the glycerol content.

Furthermore, the dc conductivity shows a thermally activated process with a well-defined activation energy,  $E_a$ , in wide temperature ranges (see Fig. 2 and Table 1); these results corroborate homogeneous or single phase film. For example, the  $G/S = 0.5$  film shows a constant phase up to approximately  $100$  °C, with a single Arrhenius-type activated process, whose activation energy is  $E_a = 0.19$  eV. Meanwhile, for the other films ( $G/S = 0.1$ – $0.4$ ), a break in the activation process is observed at around  $100$  °C that may be due to a change between two different elastomeric phases due to different content in them, as pointed out in Section 3.2. This observation is correlated with the TGA results (Fig. 5) for identical films, in which at about  $100$  °C the evaporation of water takes place under the TGA measurement conditions (open can under a flux of  $N_2$  gas). From the analysis of the TGA (Fig. 5) and DSC results (Fig. 6), the broad endothermic peaks observed in the DSC curves for all films between  $30$  and  $150$  °C under a constant  $N_2$  flux could rather be associated with the interaction starch-water-glycerol in the film. Thus, the results of  $\Delta H$  (Table 2) might be taken as the basis for evaluating the extent of interaction the G/S polymer films and water. This is so because, according to the TGA results, all the films lost an equal amount of water up to  $100$  °C ( $\sim 10$  wt %). The fact that  $\Delta H$

decreases with the increasing of the glycerol content from 10 to 40 wt % indicates that the interaction of the water molecules with the G/S polymer backbone decreases with increasing glycerol. When 50 wt % of glycerol was added,  $\Delta H$  increases again because the contribution of the enthalpy associated with the degradation of glycerol starts to be appreciable at this concentration, mainly above 100 °C. Due to the plasticizing effect of glycerol and water on the starch films, the endothermic peaks could not be associated with a melting stage of the films.

In summary, the results from partially hydrated cassava starch gelatinized membranes plasticized with appropriate content of glycerol and under controlled gas atmosphere, indicate that although water is an important factor in ionic conductivity, temperature also plays an important role in overcoming the activation barriers for ion motion, which we believe is mainly of a proton nature. Apart from a vehicular mechanism, water could also participate in the transport by a Grotthus-type mechanism transferring protons between neighboring sites provided by the glycerol [26].

## 5. CONCLUSIONS

- Our results, based on impedance spectroscopy, and thermal analysis (DSC and TGA), measurements indicate that the phase behavior of the glycerol/starch polymeric films is very sensitive to glycerol content and temperature. The dc-conductivity of the films increases with increasing both the glycerol content and temperature. The highest dc-conductivity is obtained for the G/S = 0.5 concentration, with a room temperature value at  $4.90 \text{ E-}05 \text{ Scm}^{-1}$ , and becomes thermally activated, reaching a value of  $2.13 \text{ E-}04 \text{ Scm}^{-1}$  at 100 °C.
- The dc conductivity shows thermally activated process with well defined activation energy, thus indicating homogeneous or single phase films. The G/S = 0.5 film, with the highest glycerol content, shows a constant phase up to approximately 100 °C, with a single Arrhenius-type activated process. However, for the other films (G/S = 0.1–0.4), a break is observed in the activation process at around 100 °C that may be due to a change between two different elastomeric phases with different water content in the films. These results indicate that the

water content is almost constant up to 100 °C for all film concentrations, but both the water content and the stability of the films depend strongly on having a glycerol concentration above 100 °C.

- A power-law dispersive behavior of the frequency-dependent conductivity at high frequencies has been observed in all G/S films in the blend compositions prepared, similar to that observed in other solid ionic conductors. This dispersive behavior is often referred to as “universal dynamic response.” Thus, these observations indicate charge transfer mechanisms in the G/S biopolymer system similar to those found in other ionic materials. A characteristic relaxation frequency,  $\omega_p$ , can also be defined, which marks the crossover from a low-frequency-independent region to the high-frequency dispersive region;  $\omega_p$  also appears to be thermally activated.
- The high-conducting phase found at high glycerol content and above 100 °C could open new routes for preparing promising solid electrolytes based on biopolymers, and they will be the subject of our future research program. In other words, the partially hydrated G/S polymeric systems are model compounds interesting for studying the relation between water uptake, a plasticizer effect, and ionic conductivity. Our conductivity data suggest that even after annealing and drying the materials, water takes part in the conductivity mechanisms.

## ACKNOWLEDGEMENTS

The authors are grateful for the financial support received from the *Universidad Nacional de Colombia* and DIPAL through the project-codes QUIPU 2010100772 and 2010100729. They are also grateful to Teresa Sánchez of the CIAT Palmira (Colombia) for supplying the cassava starch, and to the *Laboratorio de Nutrición Animal, Universidad Nacional de Colombia, Palmira*.

## REFERENCES

- [1] Lawton, J. W., Effect of starch type on the properties of starch containing films. *Carbohydrate Polymers*, 29, pp. 203–208, 1996.

- [2] Mathew, A. P. and Dufresne, A., Plasticized waxy maize starch: effect of polyols and relative humidity on material properties. *Biomacromolecules*, 3(5), pp. 1101–1108, 2002.
- [3] Mali, S. and Grossmann, M. V. E., Effects of yam starch films on storability and quality of fresh strawberries. *Journal of Agricultural and Food Chemistry*, 51, pp. 7005–7011, 2003.
- [4] Carvalho, A. J. F., Zambon, M. D., Curvelo, A. A. D. and Gandini, A., Thermoplastic starch modification during melt processing: hydrolysis catalyzed by carboxylic acids. *Carbohydrate Polymers*, 62, pp. 387–390, 2005.
- [5] Mina, J., Valadez, A.G., Herrera, P.F., Zuluaga, F. and Delvasto, S., Physicochemical characterization of natural and acetylated thermoplastic cassava starch. *Dyna*, 78(166), pp. 166-173, 2011.
- [6] Da Róz, A. L., Carvalho, A. J. F., Gandini, A. and Curvelo, A. A. S., The effect of plasticizers on thermoplastic starch compositions obtained by melt processing. *Carbohydrate Polymers*, 63, pp. 417–424, 2006.
- [7] Teixeira E. M., Dá Róz A. L., Carvalho, A. J. F. and Curvelo A. A. S., The effect of glycerol/sugar/water and sugar/water mixtures on the plasticization of thermoplastic cassava starch. *Carbohydrate Polymers*, 69, pp. 619–624, 2007.
- [8] Tharanathan, R. N., Starch—the polysaccharide of high abundance and usefulness. *Journal of Scientific and Industrial Research*, 54, pp. 452–458, 1995.
- [9] Tharanathan, R. N. and Saroja, N., Hydrocolloid-based packaging films, alternate to synthetic plastics. *Journal of Scientific and Industrial Research*, 60, pp. 547–559, 2001.
- [10] Riaz, M. N., Processing biodegradable packaging material from starches using extrusion technology. *Cereal Foods World*, 44, pp. 705–709, 1999.
- [11] Röper, H. and Koch, H., The role of starch in biodegradable thermoplastic materials. *Starch/Stärke*, 42, pp. 123–130, 1990.
- [12] Forssell, P. M., Mikkilä, J. M., Moates, G. K. And Parker, R., Phase and glass transition behaviour of concentrated barley starch-glycerol-water mixtures, a model for thermoplastic starch. *Carbohydrate Polymers*, 34, pp. 275–282, 1997.
- [13] Ma, X. F., Yu, J. G. and Feng, J. A., mixed plasticizer for the preparation of thermoplastic starch. *Chinese Chemical Letters*, 15(6), pp. 741–744, 2004.
- [14] Park, H.-R., Chough, S.-H., Yun, Y.-H. and Yoon, S.-D., Properties of starch/PVA blends films containing citric acid as additive. *Journal of Polymers and the Environment*, 13(4), pp. 375–382, 2005.
- [15] Zeleznak, K. J. and Hosney, R. C., The glass transition in starch. *Cereal Chemistry*, 64, pp. 121–124, 1987.
- [16] Kalichevsky, M. T. and Blanshard, J. M., The effect of fructose and water on the glass transition of amylopectin. *Carbohydrate Polymers*, 20, pp. 107–113, 1993.
- [17] Parra, D. F., Tadini C. C., Ponce P. and Lugão A. B., Mechanical properties and water vapour transmission in some blends of cassava starch edible films. *Carbohydrate Polymers*, 58, pp. 475–481, 2004.
- [18] MacCallum J. R., Vicent C. A., *Polymer electrolyte Review 1*, London Press: Elsevier Applied Science, 1987.
- [19] Gray F. M., *Polymer Electrolytes*, Cambridge: The Royal Society of Chemistry, 1997.
- [20] Gong K. C. and Cai H. S., *Solid State Ionics*, (Edited by G. Wazari, R. A. Huggins and D. F. Shriver) 377, Material Science Society, Pittsburgh, 1989.
- [21] Che, L. M., Li, D., Wang, L. J., Chen, X. D. and Mao, Z. H., Micronization and hydrophobic modification of cassava starch. *International Journal of Food Properties*, 10, pp. 527–536, 2007.
- [22] Famá, L., Flores, K. S., Gerschenson, L. and Goyanes, S., Physical characterization of cassava starch biofilms with special reference to dynamic mechanical properties at low temperatures. *Carbohydrate Polymers*, 66, pp. 8–15, 2006.
- [23] Cholwasa Bangyekan, Duangdao Aht-Ong, Kawee Srikulkit. Preparation and properties evaluation of chitosan-coated cassava starch films. *Carbohydrate Polymers*, 63, pp. 61–71, 2006.
- [24] AOAC. Official Methods of Analysis of the Association of Official Analytical Chemists. 15<sup>th</sup> Ed., Arlington, Virginia, USA. Method number 934.01, 1990.
- [25] Vargas, M. A., Vargas, R. A. and Mellander B-E., New proton conducting membranes based on PVAL/H<sub>3</sub>PO<sub>2</sub>/H<sub>2</sub>O. *Electrochimica Acta*, 44, pp. 4227–4232, 1999.
- [26] ASTM. Standard test method for transition temperatures of polymers by differential scanning calorimetry D3418. In: *Annual book of ASTM*, Vol. 08.02. Philadelphia: ASTM, 2005.

[27] Castillo, J., Cachón, M., Delgado, I. and Vargas, R. A., New Solid Ionic Conductor Base on Poly(ethylene oxide) and Sodium Trifluoroacetate. *Electrochimica Acta*, 46, pp. 1695–1697, 2001.

[28] Castillo, J., Materón, E.M., Castillo, R., Vargas, R.A., Bueno, P.R. and Varela, J.A. Electrical relaxation in proton conductor composites base on  $(\text{NH}_4)\text{H}_2\text{PO}_4/\text{TiO}_2$ . *Ionics*, 15, pp. 329–336, 2009.

[29] Funke, K., Jump Relaxation in Solid Electrolytes. *Progress in Solid State Chemistry*, 22, pp. 111–195, 1993.

[30] Müller, C. M.O., Yamashita, F. and Borges, J. L., Evaluation of the effects of glycerol and sorbitol concentration and water activity on the barrier properties of cassava starch films thought a solubility approach. *Carbohydrate Polymers*, 72, pp. 82–87, 2008.